EDITOR'S CHOICE

Evaluation of Articular Surface Similarity of Hemi-Hamate Grafts and Proximal Middle Phalanx Morphology: A 3D Geometric Morphometric Approach

David R. Sollaccio, MD,*¶ Paul Navo, MPH, BS,* Alidad Ghiassi, MD,* Caley M. Orr, PhD,§‖ Biren A. Patel, PhD,†‡ Kristi L. Lewton, PhD†‡

Purpose Hemi-hamate arthroplasty has been described as a viable treatment option for unstable proximal interphalangeal joint fracture-dislocations. The procedure uses a dorsal distal hamate osteochondral graft to recreate the injured volar middle phalanx (MP) proximal base. The purpose of this study was to evaluate the similarity in shape of these articular surfaces using quantitative 3-dimensional methods.

Methods Three-dimensional virtual renderings were created from laser scans of the articular surfaces of the dorsal distal hamate and the volar MP bases of the index, middle, ring, and little fingers from cadaveric hands of 25 individuals. Three-dimensional landmarks were obtained from the articular surfaces of each bone and subjected to established geometric morphometric analytical approaches to quantify shape. For each individual, bone shapes were evaluated for covariation using 2-block partial least-squares and principal component analyses.

Results No statistically significant covariation was found between the dorsal distal hamate and volar MP bases of the middle, ring, or little digits. Whereas the volar MP bases demonstrated relative morphologic uniformity among the 4 digits both within and between individuals, the dorsal distal hamates exhibited notable variation in articular surface morphology.

Conclusions Despite the early to midterm clinical success of hemi-hamate arthroplasty, there is no statistically significant, uniform similarity in shape between the articular surfaces of the dorsal distal hamate and the volar MP base. In addition, there is wide variation in the articular morphology of the hamate among individuals.

Clinical relevance The lack of uniform similarity in shape between the dorsal distal hamate and the volar MP base may result in unpredictable outcomes in HHA. It is recommended that the variation in hamate morphology be considered while reconstructing the injured volar MP base in the procedure. *(J Hand Surg Am. 2019;44(2):121−128. Copyright © 2019 by the American Society for Surgery of the Hand. All rights reserved.)*

Key words Anatomic, hemi-hamate arthroplasty, osteochondral autograft, proximal interphalangeal joint dislocation, proximal interphalangeal joint fracture.

*From the *Department of Orthopaedic Surgery and †Department of Integrative Anatomical Sciences, Keck School of Medicine; and the ‡Human and Evolutionary Biology Section, Department of Biological Sciences, University of Southern California, Los Angeles, CA; and the §Department of Cell and Developmental Biology, University of Colorado School of Medicine, Aurora; and ‖Department of Anthropology, University of Colorado Denver, Denver, CO.*

¶Dr. Sollaccio is currently affiliated with the Department of Orthopaedic Surgery, Southern California Permanente Medical Group, Woodland Hills, CA.

Received for publication August 14, 2017; accepted in revised form May 25, 2018.

No benefits in any form have been received or will be received related directly or indirectly to the subject of this article.

Corresponding author: David R. Sollaccio, MD, Department of Orthopaedic Surgery, Southern California Permanente Medical Group, Woodland Hills Medical Center, 5601 De Soto Avenue, Woodland Hills, CA 91368; e-mail: davidrsollaccio@gmail.com.

0363-5023/19/4402-0005$36.00/0
https://doi.org/10.1016/j.jhsa.2018.06.008

Proximal interphalangeal (PIP) joint fracture-dislocations are problematic injuries with a propensity for developing long-term morbidity such as chronic stiffness, pain, and abnormal joint motion. For this reason, appropriate and expedient treatment is critical to restoring function. Although many treatment techniques have been proposed, it is accepted that fundamental goals should be to obtain and maintain a smooth, congruous articular surface and initiate early, active motion of the PIP joint.[1,2] A practical surgical technique to achieve this goal is the hemi-hamate arthroplasty (HHA). Initially presented by Hastings and colleagues (at the 54th annual meeting of the American Society for Surgery of the Hand, 1999), HHA is a procedure in which an autologous, osteochondral graft is harvested from the distal articular surface of the hamate and then used to recreate the volar base of the middle phalanx (MP).

Outcome studies have shown that HHA can yield an average of 77° PIP joint motion and 91% grip strength (compared with the healthy contralateral side) at final postoperative follow-up among both acute and chronic injuries.[3–10] Although the procedure demonstrates reasonable success in return of short-term function, it poses a risk for complications such as up to a 50% long-term rate of PIP joint radiographic osteoarthrosis.[3,5–8,10] The incidence of radiographic osteoarthrosis is considerable, but the degree to which this affects long-term functional outcomes remains unclear.

There has been recent interest in using advanced imaging modalities to refine the technique of HHA. Calva et al[11] examined computed tomography (CT) scans to determine the anatomical consistency between the distal hamate and MP base using angular and linear measurements in the coronal plane. Other studies have used CT imaging to investigate the HHA technique in 3 dimensions, but with a specific focus on a particular approach to graft harvest[12] or the ideal positioning of the graft in the recipient bed.[13] The aim of this study was to use a quantitative anatomical approach that analyzed 3-dimensional (3D) shape to compare the dorsal distal hamate and the volar MP base. Specifically, we tested the null hypothesis that the shapes of their articular surfaces were similar.

MATERIALS AND METHODS

The osteological sample was derived from the cadaveric specimens of 25 adult individuals (12 males and 13 females) from the Raymond A. Dart Collection (in the Hunterian Museum of Anatomy of the University of the Witwatersrand [Johannesburg, South Africa]) and the Terry Collection (in the Department of Anthropology of the US National Museum of Natural History [Washington, DC]). Three-dimensional virtual surface renderings were created of isolated hamates and the middle phalanges of the index (MP2), middle (MP3), ring (MP4), and little (MP5) fingers from the same hand using a 3D laser scanner (NextEngine, Inc, Santa Monica, CA) following the approach taken in other studies.[14,15] Scans were obtained with a resolution of greater than 10,000 points per square inch, and 6 to 9 scans were taken at different positions and then merged using ScanStudio HD PRO software (NextEngine, Inc) and saved as .PLY files. Any scanning defects in the mesh surface models were corrected using Geomagic Studio software (version 12, 3D Systems, Inc, Rock Hill, SC; 2010). In this study, we targeted right-side hand bones for data collection, but when only left-side bones were available, the virtual left-side bones were mirror-imaged to their antimere.

We used 3D geometric morphometric methods in this study because they are ideal for analyzing complex 3D bone shapes. These methods use xyz coordinates of anatomical landmarks to quantify overarching shape patterns and are well-suited to answering questions about patterns of covariation between bone surfaces.[16–18] In this study, covariations in shape between the hamate's distal articular surface (H_{DAS}) and the MP's proximal articular surface (MP_{PAS}) were compared. For each virtual bone, a patch of 17 × 17 3D landmarks were placed using Checkpoint software (Stratovan Corp, Davis, CA). The landmark patch was placed on the dorsal half of the H_{DAS} and the volar half of MP_{PAS} (Fig. 1); the dorsovolar height of the landmark patch was 50% of the articular surface height. The patch consisted of 17 fixed landmarks (shown in red in Fig. 1) and 272 semilandmarks (shown in gold in Fig. 1). Fixed landmarks were placed at homologous regions along the ulnar, radial, and dorsal (for the hamates) or volar (for the phalanges) margins of the articular surface, and radioulnarly across the articular surface along the 50% line (resected edge in Fig. 1). All landmarks were placed by a single observer and intraobserver measurement error analysis was conducted for one hamate and one MP2. The landmark set was placed 8 times on each bone and mean measurement error (measured as the mean of the percent deviation of each replicate from the replicate mean) was 3.2% for the hamate and 4.6% for MP2.

Each bone-specific landmark data set was aligned using generalized Procrustes analysis, which scales, rotates, and translates each individual landmark configuration to remove the effects of size and

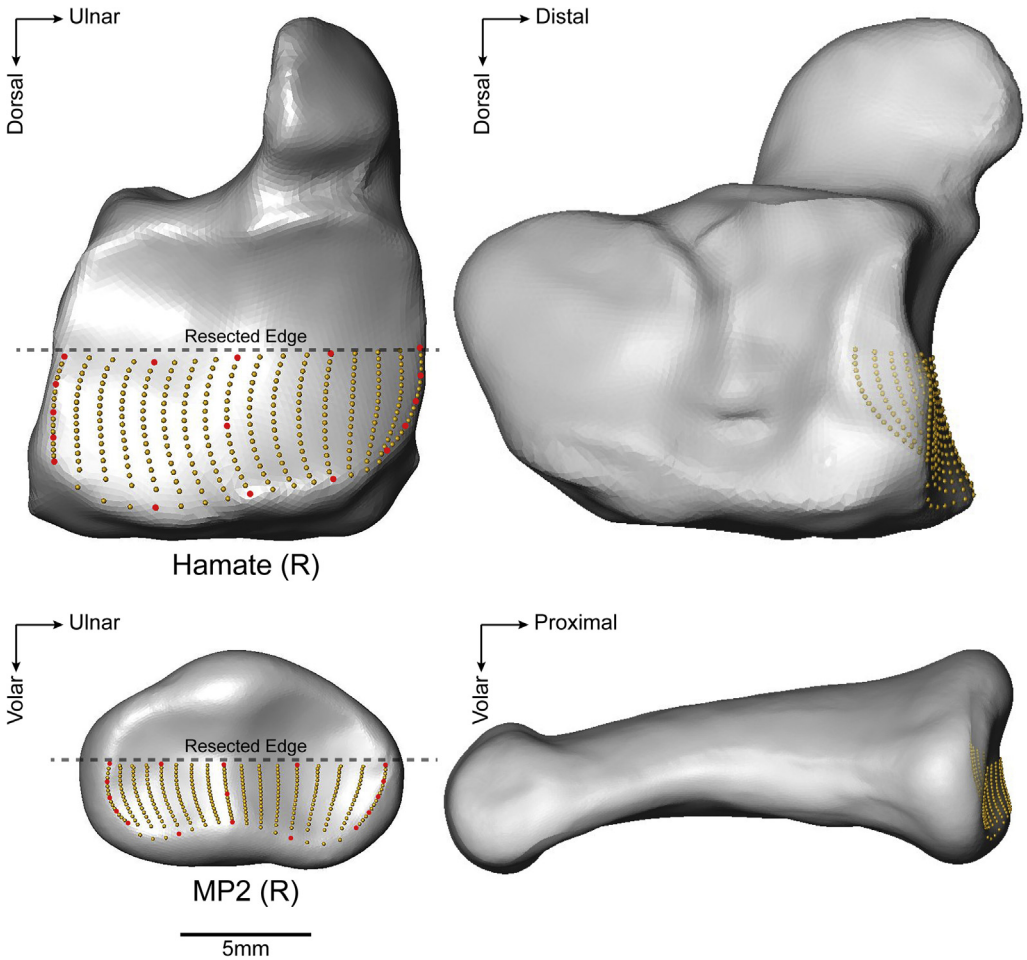

FIGURE 1: Surfaces of a hamate and index middle phalanx (MP2) overlain with the 3D landmark patch. The dotted line indicates 50% of the height of the articular surface. Gold landmarks are sliding semilandmarks; red landmarks are fixed type II and III landmarks.

orientation differences.[19] Semilandmarks located along the articular margin were allowed to slide along the curve, whereas semilandmarks located on the articular surface were allowed to slide along the surface; sliding along tangent directions was performed using Procrustes distances.[20] Subsequent analyses were performed on Procrustes-aligned landmark coordinates. All analyses were performed in the Geomorph package (version 3.0.4)[21,22] for R (version 3.4.1).[23]

To test whether landmarked regions of the H_{DAS} and MP_{PAS} covaried in 3D shape, a 2- block partial least-squares (2B-PLS) analysis was performed for each hamate−MP pair (ie, hamate−MP2, hamate−MP3, etc). This analysis compared covariation in 2 sets of variables (using singular value decomposition of the covariance matrix) and constructed linear combinations of the variables that accounted for maximum covariation between the original variables.[19] This method is common in 3D geometric morphometry when examining the degree of covariation between apposing joint surfaces,[16,18] among and between cranial and postcranial bones,[17,24] and between morphology and other variables such as geography.[25] The 2B-PLS analysis yields a correlation coefficient (r) between the 2 blocks and a significance value (*P*) obtained using a permutation test. Simply stated, a statistically significant result of the test indicates that the 2 shapes of interest are similar.

To visualize variations in H_{DAS} and MP_{PAS} shape, we performed a principal component analysis. Resulting eigenvalues were examined to determine the proportion of variation explained by the principal components (PC). A power analysis was performed to demonstrate that the sample size was sufficient to detect statistical significance. Power ranged from 86% with the MP2 analysis to 97% with the MP3 analysis, indicating a risk of type II error ranging from 3 to 14% (Table 1).

RESULTS

Results of the 2B-PLS analysis demonstrated that H_{DAS} and MP2-5_{PAS} did not covary (ie, *P* values for all 4

TABLE 1. Two-Block Partial Least-Squares Results for Comparisons of Hamate Versus Each MP

MP	n	r	*P*	Power
2	23	0.58	.81	.86
3	24	0.68	.39	.97
4	25	0.62	.92	.93
5	24	0.61	.82	.91

n represents the number of bone specimens.

comparisons were not statistically significant) (Table 1). The plot of PC1 on PC2 scores further demonstrated this lack of correlation between the articular surface morphology of the hamate and the middle phalanx (Fig. 2). On PC1 (which accounted for 35.1% of the sample variation), there was separation between H_{DAS} that aligned toward the negative side of the axis and the MP2-5_{PAS} that aligned more on the positive side; the MPs clustered together in shape space and could not be distinguished from each other. In the distal view, the H_{DAS} was expanded dorsovolarly and its dorsal articular margin was U-shaped. In the profile view, with the hamate rotated 90° dorsally away from the viewer, the H_{DAS} tended to be S-shaped; the radial articular surface for the fifth metacarpal base was concave and the ulnar articular surface for the fourth metacarpal base was more convex. The MP_{PAS} had a horizontally rotated, B-shaped articular margin in which the length of the median articular ridge was shorter than the ulnar and radial aspects of the articular rim. In the profile view, with the MP rotated 90° dorsally away from the viewer, the MP_{PAS} was W-shaped; both ulnar and radial sides of the articular surface area were concave distally.

Variations in PC2 (accounting for 18.3% of sample variation) explain variations in the ulnar versus radial expansion of the articular surfaces as well as the depth of the articular surfaces relative to the position of the median articular ridge on both hamates and MPs. On the positive end of PC2, articular surfaces were more expanded radially and shallow proximodistally, whereas on the negative end they were expanded more ulnarly and deep proximodistally (Fig. 2).

A notable aspect of the principal component analysis results was the large amount of shape variation exhibited by H_{DAS}. In contrast, the MP2-5_{PAS} were less variable in their shapes. To illustrate the variation in hamates, 3 individuals were qualitatively compared: one from the negative extreme on PC1 (Fig. 3A), one from the middle of the hamate cluster representing an average morphology (Fig. 3B), and one from the positive end of the hamate group (Fig. 3C). In the distal view, both the individual from the negative end of PC1 and the individual representing the average shape had dorsovolarly expanded articular surfaces relative to their MP2 (and MP3 to 5, which are not shown). Also, in the profile view, both exhibited the S-shaped articular surface, compared with the W-shaped articular surface of their corresponding MPs. The individual with the most positive PC1 score, which plotted closest to the MPs, generally exhibited a morphology that was more phalanx-like, with less dorsovolar expansion in the proximal view and less convexity of the ulnar articular surface in the profile view.

DISCUSSION

Hemi-hamate arthroplasty has been proposed as a practical treatment option for unstable PIP joint fracture-dislocations in both the acute and chronic settings.[3−10] The primary goal of HHA is to recreate a stable volar lip of the base of the proximal phalanx.[6,10,26] It has been suggested that there is an inherent anatomical similarity between the articular surfaces of the dorsal distal hamate and the volar MP base.[9]

The results presented here suggest that the morphological relationship between the MP_{PAS} and the H_{DAS} is more complex than previously appreciated. In their study, Calva et al[11] determined that there were inconsistencies between the 2 joint surfaces based on 2D CT measurements. They found overall low angular and linear consistency between the hamate and middle phalanx bases, with the most consistency found in the little finger (38.7%) and the least consistency in the index finger (12.9%). Our findings expand on this important point by demonstrating that there is a lack of uniform morphologic similarity between the MP_{PAS} and the H_{DAS} when measured in 3D space (Fig. 2). Specifically, our results demonstrated that whereas all 4 MPs were similar in shape, hamates generally had dorsovolarly expanded articular surfaces that were S-shaped in the profile view and did not overlap with MPs (Fig. 2). Furthermore, there was substantial variation in hamate morphology among individuals. Finally, whereas the results of Calva et al demonstrated variation in the similarity of hamate−MP joint surfaces depending on the specific digit examined, our results showed that all MP_{PAS} were remarkably similar in 3D shape and that no one digit demonstrated improved covariation with the dorsal distal hamate compared with the others (Fig. 2).

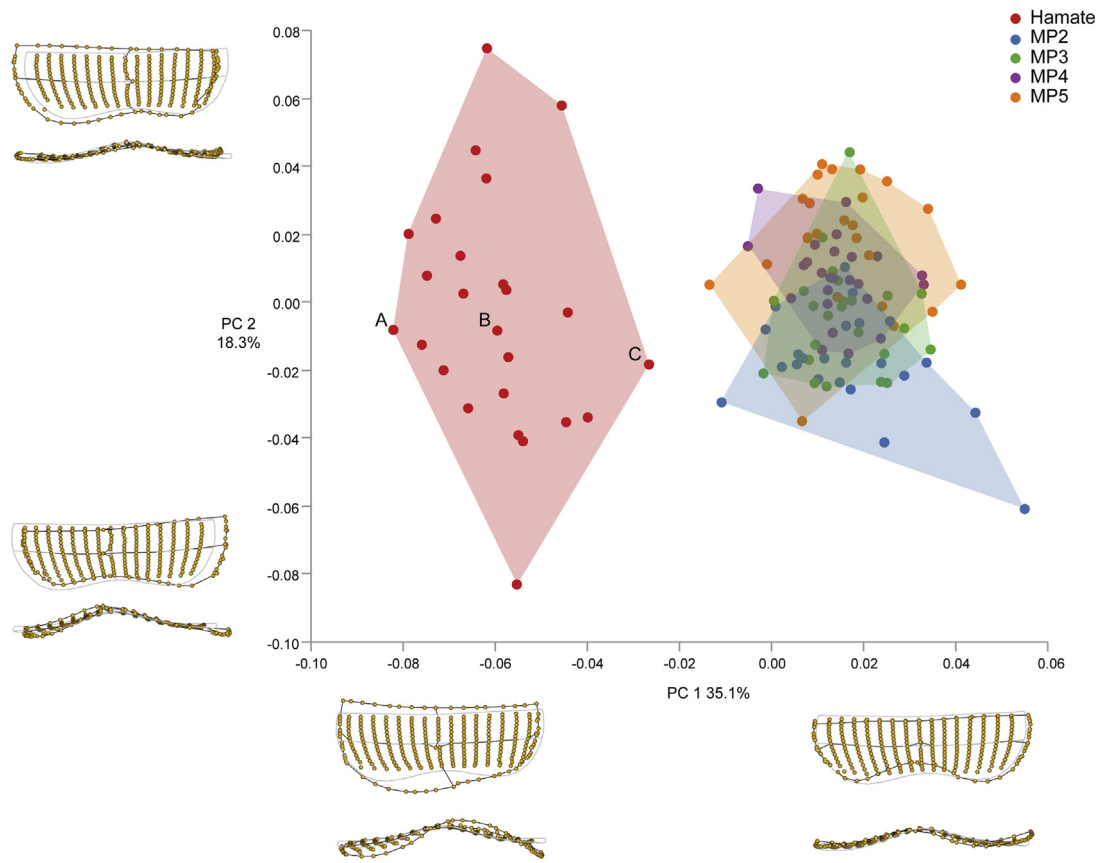

FIGURE 2: Bivariate plot of PC1 on PC2. Wireframes at the positive and negative ends of PCs 1 and 2 indicate the extremes of morphology on each axis. Landmarks are connected by black wireframe links to create outlines that improve visualization and show the deviation from the whole-sample mean shape (light gray outlines within the wireframes). For each of the 4 wireframe images, the top view is the full articular surface view (distal on hamates and proximal on middle phalanges [MP2-5]) and the bottom view is the profile view with the bone rotated 90° dorsally away from the viewer. Within the red hamate region of the plot, individuals labeled A, B, and C correspond to those with the most negative, average, and most positive PC1 scores. Figure 3 compares the morphology of these individuals.

Several limitations of our study are worth noting. First, our study population consisted of 25 hand specimens. We performed a power analysis, which demonstrated an adequate sample size to achieve a risk of type II error of less than 20% (Table 1). However, considering the amount of shape variation within our sample, particularly among the hamate articular surfaces, future studies with larger sample sizes obtained from additional populations may provide more information about the ranges in variation in morphology of the volar MP base and the dorsal distal hamate. Second, although we examined each specimen model visually for articular irregularities, it is unclear whether there were any subtle degenerative or posttraumatic osteological changes in the articular surfaces that may have influenced our results. In addition, our study used skeletal specimens without ligamentous, cartilaginous, or other soft tissues; as a result, our 3D models approximated the topography of the subchondral bone rather than the articular cartilage itself. Although it is well-known that the articular cartilage of the distal hamate is thicker than that of the MP base,[9] the hyaline cartilage should exhibit a topography similar to that of its underlying bone in healthy specimens, and therefore the same conclusion would be expected. Finally, we analyzed the dorsal half of the hamate articular surface and the volar half of the middle phalanx base articular surface. This resected edge was chosen for the purposes of standardization and reproducibility. We acknowledge that in the clinical setting, PIP joint fracture-dislocations can yield articular surface defects that do not precisely match the areas of measurement in our study. We also acknowledge that the distal hamate osteochondral grafts are typically adjusted by the surgeon at the time of implantation to best restore joint stability, and that this could not be accounted for in our study.

FIGURE 3: Hamate shape variation along PC1 exemplified by Procrustes-aligned coordinates of 3 individuals. Hamate in the first column and index middle phalanx (MP2) in the second column. The first row of each panel shows full articular surface views whereas the second row shows profile views (in the hamate this is dorsal to volar; in the phalanx this is volar to dorsal). **A** The individual with the most negative PC1 scores (Dart number 493); **B** the individual with average PC1 scores (US National Museum of Natural History number 561); and **C** the individual with the most positive PC1 scores (Dart number 3120). These individuals are also shown in Figure 2. Because these are Procrustes-aligned coordinates, all bones are scaled to the same size. Orientations as in Figure 1.

Strengths of our study lie in its use of quantitative methods of 3D shape analysis to capture the complex shape of the entire volar 50% of the MP base (thereby recreating an unstable fracture-dislocation) and the dorsal distal hamate used in osteochondral grafts. This approach allowed us to test the covariation between hamate and MP morphology using the entire 3D shape of the articular surfaces, as opposed to merely linear or angular measurements, as were previously documented. This is an improvement on

previous work because it gives a more detailed understanding of hamate−MP differences in articular surface shape (including the degree of lipping of the articular margins). Finally, our inclusion of MP bases and the ipsilateral distal hamate from the same donor optimized the translational application of our results, particularly given the variation in articular surface morphology among subjects.

Our study demonstrates that the 3D articular morphologies of the MP_{PAS} and the H_{DAS} are not as similar as they appear on 2D radiographic imaging. Moreover, there is significant variability in the H_{DAS} morphology among individuals. Bearing in mind the considerable rate of postoperative radiographic osteoarthrosis and the lack of clinical studies assessing long-term outcomes in HHA, it may be that this lack of shape similarity between donor and recipient joint surfaces influences joint mechanics and the development of subsequent arthrosis. It may also be that individuals with varying H_{DAS} morphology might expect different postoperative outcomes after HHA. The finding of hamate variation (Fig. 3) highlights that whereas some individuals have H_{DAS} that more closely resemble MP_{PAS}, others may not. However, according to Ng and Watts,[27] the properties of an ideal autograft are simply the provision of mechanical stability, the long-lasting anatomical reconstruction of the joint surface, and the mitigation of donor site morbidity. Therefore, it is possible that the differences we found in articular surface morphology bear no important impact on the goals of HHA and its long-term clinical outcomes. Nevertheless, the morphologic variability of the hamate osteochondral graft warrants consideration when performing HHA.

ACKNOWLEDGMENTS

This work was supported in part by the National Science Foundation (Grant Numbers BCS-1317041 to BAP and BCS-1539741 to CMO). Thank you to David Hunt (Smithsonian Institution) and Brendon Billings (University of Witwatersrand) for facilitating access to the Terry and Dart skeletal collections, respectively. Thank you to Avery Williams for scanning the osteological specimens from the Dart Collection at the University of the Witwatersrand.

REFERENCES

1. Freiberg A, Pollard BA, Macdonald MR, Duncan MJ. Management of proximal interphalangeal joint injuries. *Hand Clin*. 2006;22(3):235−242.
2. McAuliffe JA. Dorsal fracture dislocation of the proximal interphalangeal joint. *J Hand Surg Am*. 2008;33(10):1885−1888.
3. Afendras G, Abramo A, Mrkonjic A, Geijer M, Kopylov P, Tagil M. Hemi-hamate osteochondral transplantation in proximal interphalangeal dorsal fracture dislocations: a minimum 4 year follow-up in eight patients. *J Hand Surg Eur Vol*. 2010;35(8):627−631.
4. Bigorre N, Rabarin F, Jeudy J, Cesari B. Hemi-hamate arthroplasty reconstruction for chronic proximal interphalangeal fracture-dislocation. *Chir Main*. 2014;33(2):148−152.
5. Calfee RP, Kiefhaber TR, Sommerkamp TG, Stern PJ. Hemi-hamate arthroplasty provides functional reconstruction of acute and chronic proximal interphalangeal fracture-dislocations. *J Hand Surg Am*. 2009;34(7):1232−1241.
6. Frueh FS, Calcagni M, Lindenblatt N. The hemi-hamate autograft arthroplasty in proximal interphalangeal joint reconstruction: a systematic review. *J Hand Surg Eur Vol*. 2015;40(1):24−32.
7. Korambayil PM, Francis A. Hemi-hamate arthroplasty for pilon fractures of finger. *Indian J Plast Surg*. 2011;44(3):458−466.
8. Rozen WM, Niumsawatt V, Ross R, Leong JC, Ek EW. The vascular basis of the hemi-hamate osteochondral free flap. Part 1: vascular anatomy and clinical correlation. *Surg Radiol Anat*. 2013;35(7):595−608.
9. Williams RM, Kiefhaber TR, Sommerkamp TG, Stern PJ. Treatment of unstable dorsal proximal interphalangeal fracture/dislocations using hemi-hamate autograft. *J Hand Surg Am*. 2003;28(5):856−865.
10. Yang DS, Lee SK, Kim KJ, Choy WS. Modified hemihamate arthroplasty technique for treatment of acute proximal interphalangeal joint fracture-dislocations. *Ann Plast Surg*. 2014;72(4):411−416.
11. Calva D, Culotta N, Lopez J, et al. A simple pre-operative imaging method to assess donor and recipient anatomy in hemi-hamate arthroplasty for proximal interphalangeal joint reconstruction. *Surg Radiol Anat*. 2016;38(6):699−704.
12. Ten Berg P, Ring D. Quantitative 3D-CT anatomy of hamate osteoarticular autograft for reconstruction of the middle phalanx base. *Clin Orthop Relat Res*. 2012;470(12):3492−3498.
13. Shih J, Podolsky D, Binhammer P. Three-dimensional remodeling to determine best fit for hemihamate autograft arthroplasty. *Plast Surg (Oakv)*. 2014;22(3):191−195.
14. Almécija S, Orr CM, Tocheri MW, Patel BA, Jungers WL. Exploring phylogenetic and functional signals in complex morphologies: the hamate of extant anthropoids as a test case study. *Anat Rec (Hoboken)*. 2015;298(1):212−229.
15. Patel BA, Yapuncich GS, Tran C, Nengo IO. Catarrhine hallucal metatarsals from the early Miocene site of Songhor, Kenya. *J Hum Evol*. 2017;108:176−198.
16. Harcourt-Smith WEH, Tallman M, Frost SR, Wiley DF, Rohlf FJ, Delson E. Analysis of selected hominoid joint surfaces using laser scanning and geometric morphometrics: a preliminary report. In: Sargis EJ, Dagosto M, eds. *Mammalian Evolutionary Morphology: A Tribute to Frederick S. Szalay*. New York, NY: Springer; 2008:373−383.
17. Tallman M. Forelimb to hindlimb shape covariance in extant hominoids and fossil hominins. *Anat Rec (Hoboken)*. 2013;296(2):290−304.
18. Turley K, Frost SR. The appositional articular morphology of the talo-crural joint: the influence of substrate use on joint shape. *Anat Rec (Hoboken)*. 2014;297(4):618−629.
19. Rohlf FJ, Corti M. Use of two-block partial least-squares to study covariation in shape. *Syst Biol*. 2000;49(4):740−753.
20. Gunz P, Mitteroecker P. Semilandmarks: a method for quantifying curves and surfaces. *Hystrix*. 2013;24(1):103−109.
21. Adams DC, Collyer ML, Kaliontzopoulou A, Sherratt E. Geomorph: software for geometric morphometric analyses. R package version 3.0.4. Available at: http://cran.rproject.org/web/packages/geomorph/index.html. Accessed August 14, 2017.
22. Adams DC, Otárola-Castillo E. Geomorph: an R package for the collection and analysis of geometric morphometric shape data. *Methods Ecol Evol*. 2013;4(4):393−399.

23. R Core Team. R: A language and environment for statistical computing. R Foundation for Statistical Computing, Vienna, Austria. Available at: https://www.R-project.org/. Accessed August 14, 2017.
24. Bookstein FL, Gunz P, Mitteroecker P, Prossinger H, Schaefer K, Seidler H. Cranial integration in Homo: singular warps analysis of the midsagittal plane in ontogeny and evolution. *J Hum Evol*. 2003;44(2):167−187.
25. Frost SR, Marcus LF, Bookstein FL, Reddy DP, Delson E. Cranial allometry, phylogeography, and systematics of large-bodied papionins (Primates: Cercopithecinae) inferred from morphometric analysis of landmark data. *Anat Rec A Discov Mol Cell Evol Biol*. 2003;275(2):1048−1072.
26. McAuliffe JA. Hemi-hamate autograft for the treatment of unstable dorsal fracture dislocation of the proximal interphalangeal joint. *J Hand Surg Am*. 2009;34(10):1890−1894.
27. Ng CY, Watts AC. The use of non-vascularised osteochondral autograft for reconstruction of articular surfaces in the hand and wrist. *J Bone Joint Surg Br*. 2012;94(11):1448−1454.